Electronic Supplementary Information

Multifunctional Nanocomposite Structural Separators for Energy Storage

Luiz Acauan [a], Yue Zhou [a], Estelle Kalfon-Cohen [a], Nathan K. Fritz [b] and Brian L. Wardle [a]**

[a] Department of Aeronautics and Astronautics, Massachusetts Institute of Technology, 77 Massachusetts Ave., Cambridge, Massachusetts 02139, USA

[b] Department of Mechanical Engineering, Massachusetts Institute of Technology, 77 Massachusetts Ave., Cambridge, Massachusetts 02139, USA

*Email: lacauan@mit.edu; wardle@mit.edu

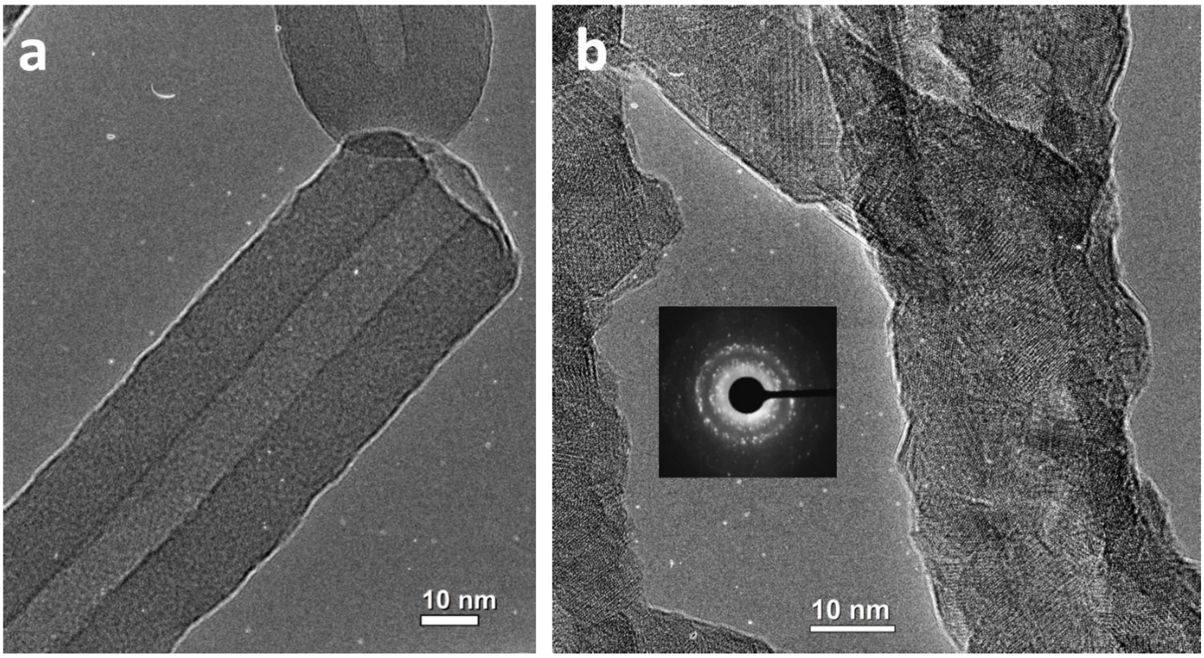

Fig. S1. Transmission electron microscopy (TEM) images: **a)** Amorphous alumina nanotube (ANT) after 550 °C treatment in air. At this temperature, carbon nanotubes (CNTs) slowly burn and are completely removed without collapsing the alumina outer shell; and **b)** polycrystalline ANTs after 1050 °C treatment in air. The image shows clear fringes related to the crystal lattice of the multiple grains in the ANT. The inset in **b** shows the electron diffraction pattern with multiple diffraction dots confirming polycrystallinity.

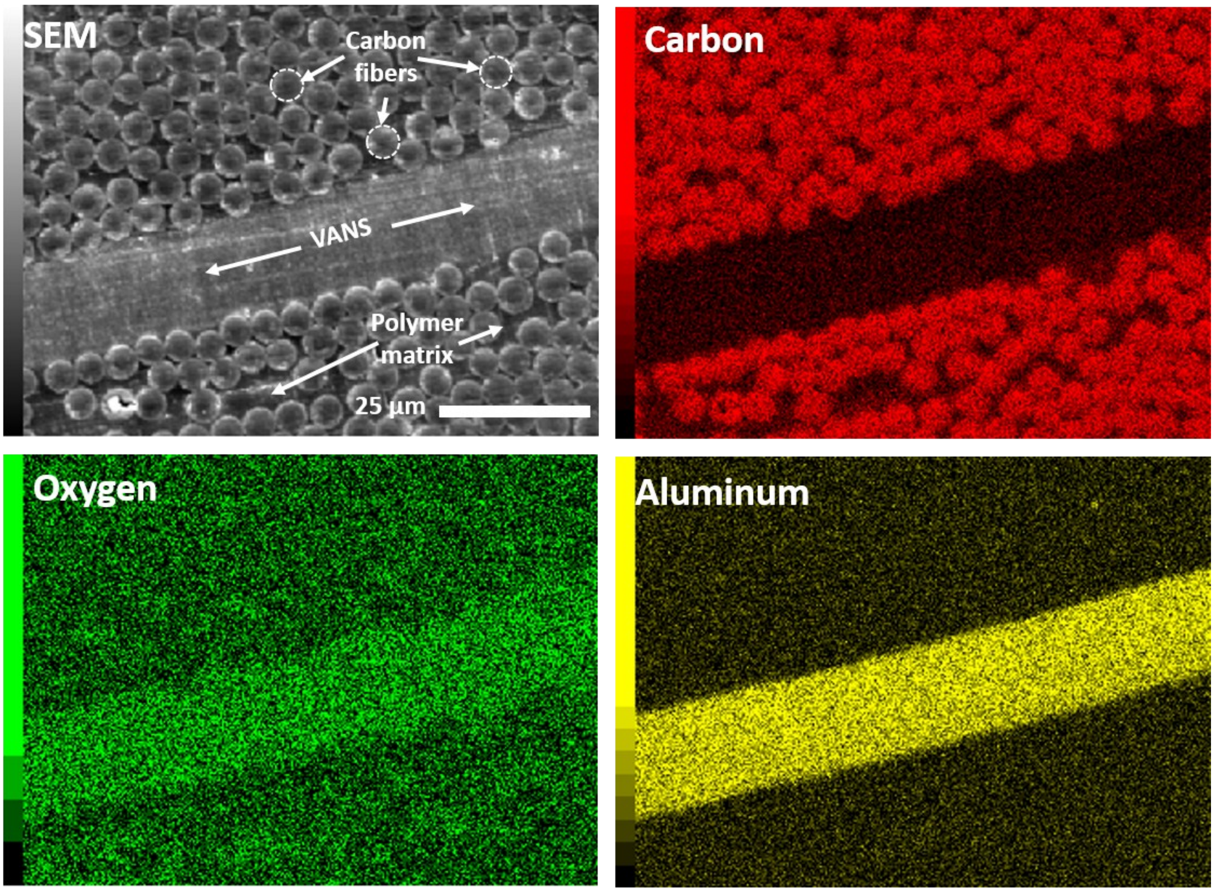

Fig. S2. Energy Dispersive Spectroscopy **(EDS)** mapping of VANS cross-section from carbon, oxygen and aluminum, the carbon map shows similar intensity of carbon in the VANS region as in the polymer regions in between carbon fibers, indicating polymer infusion into the ANTs. The Oxygen and Aluminum images display the intense signal coming from the VANS related to the Al_2O_3 composition of the ANTs.

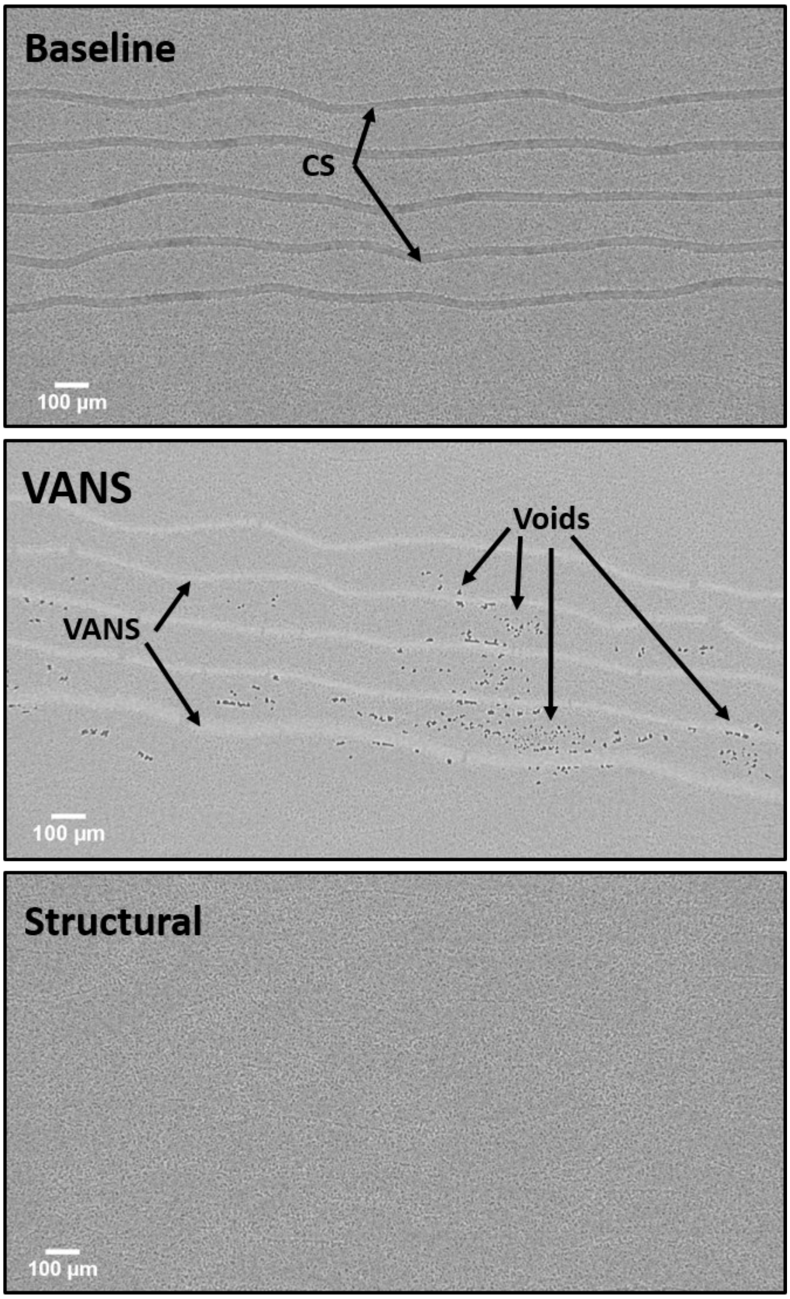

Fig. S3. µCT scans from Baseline, VANS, and Structural composites. Structural is a unidirectional composite which does not reveal clear interfaces from ply to ply. Baseline and VANS have their interlaminar regions well defined by the introduction of the separators with no apparent voids within the interlaminar region, although the VANS specimen has voids distributed inside of the laminae (0.28% ±0.14).

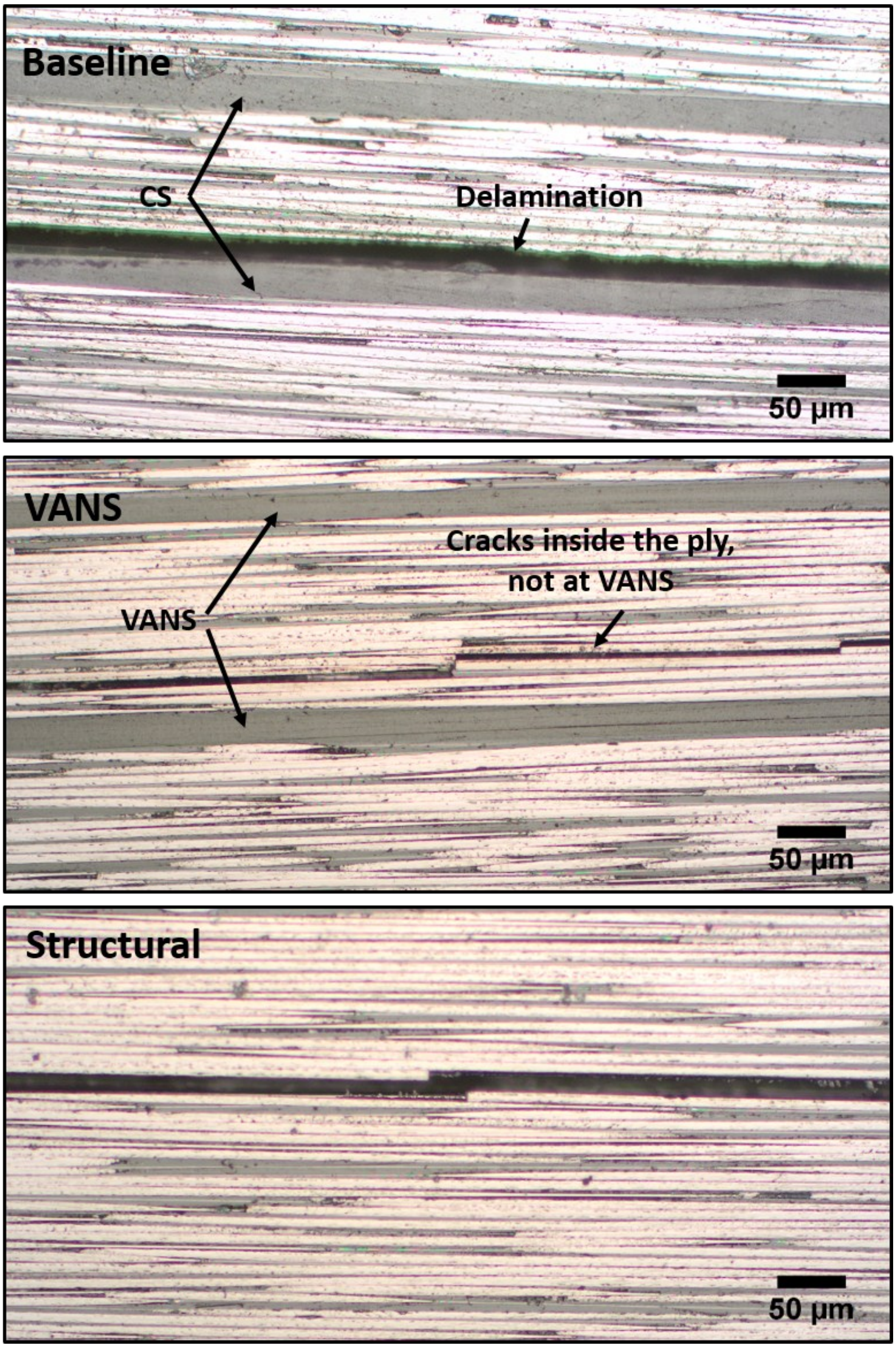

Fig. S4. *Post-mortem* optical cross-sectional images after failure during short beam shear testing of the Baseline, VANS, and Structural composites. Unidirectional carbon fibers run horizontally in the images. All Baseline samples have the CS exposed in one of the halves of the broken composites, showing a clear failure by interface delamination. In VANS composites, cracks initiate at the VANS/laminae interface or within the ply, but always propagate inside the ply (intralaminar, vs. interlaminar cracks). The aligned ANTs "stitch" the laminates together, enhancing interlaminar shear strength and forcing damage into the ply and away from the interface.

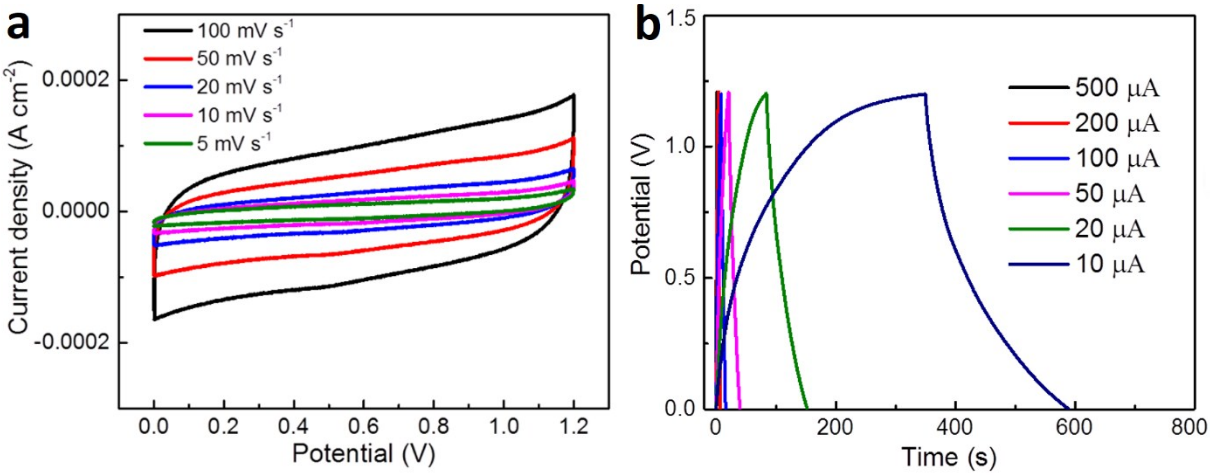

Fig. S5. (a) Cyclic voltammetry (CV) curves of the cell based on P(VDF-HFP)/ANTs composite separator at different scan rates of 100, 50, 20, 10, and 5 mV s^{-1}, respectively. The curve at 100 mV s^{-1} presented here was compared with the performance of the cell with pure P(VDF-HFP) separator at the same scan rate and is displayed in Figure 4e. (b) Galvanostatic charging and discharging performance of the cell based on P(VDF-HFP)/ANTs composite separator at different currents of 500, 200, 100, 50, 20, and 10 μA, respectively. The specific capacitance can be calculated via $C = \frac{I/A}{\Delta V/\Delta t} * 4$, where I is the current, A is the area of electrode, ΔV is the potential difference in the discharge curve, and Δt is the time difference in the discharge curve. The calculation and the specific capacitance with different currents is shown in Figure 4f.

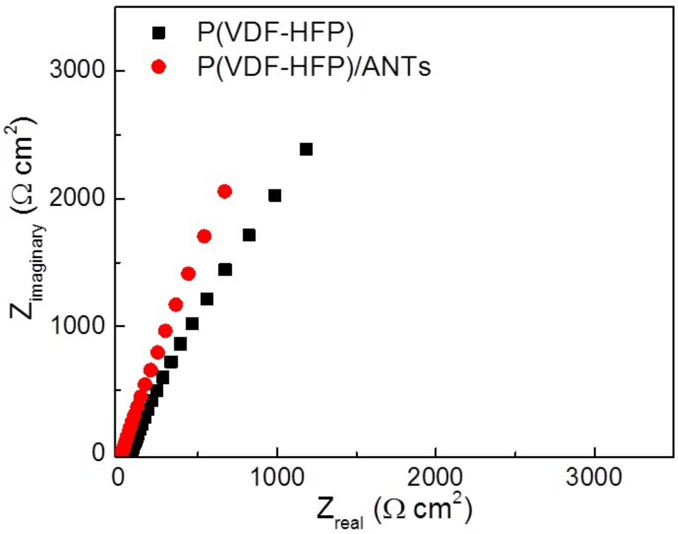

Fig. S6. The Nyquist plots of cells with P(VDF-HFP)/ANTs composite separator and pure P(VDF-HFP) separator, respectively. The frequency range was set from 1 MHz to 100 mHz at open circuit potential with a 5 mV perturbation signal. The cell with composite separator exhibits much smaller resistance (Z_{real}) compared with that of cell with pure polymer separator.